A MOVPE method for improving InGaN growth quality by pre-introducing TMIn

Zi-Kun Cao(曹子坤), De-Gang Zhao(赵德刚), Jing Yang(杨静), Jian-Jun Zhu(朱建军), Feng Liang(梁锋), and Zong-Shun Liu(刘宗顺)

Citation: Chin. Phys. B, 2021, 30 (**1**): 018103. DOI: 10.1088/1674-1056/abb801
Journal homepage: http://cpb.iphy.ac.cn; http://iopscience.iop.org/cpb

What follows is a list of articles you may be interested in

Carrier transport via V-shaped pits in InGaN/GaN MQW solar cells

Shitao Liu(刘诗涛), Zhijue Quan(全知觉), Li Wang(王立)
Chin. Phys. B, 2017, 26 (**3**): 038104. DOI: 10.1088/1674-1056/26/3/038104

Superior material qualities and transport properties of InGaN channel heterostructure grown by pulsed metal organicchemical vapor deposition

Ya-Chao Zhang(张雅超), Xiao-Wei Zhou(周小伟), Sheng-Rui Xu (许晟瑞), Da-Zheng Chen(陈大正), Zhi-Zhe Wang(王之哲), Xing Wang(汪星), Jin-Feng Zhang(张金风), Jin-Cheng Zhang(张进成), Yue Hao(郝跃)
Chin. Phys. B, 2016, 25 (**1**): 018102. DOI: 10.1088/1674-1056/25/1/018102

Growth and fabrication of semi-polar InGaN/GaN multi-quantum well light-emitting diodes on microstructured Si (001) substrates

Chen Long, Payne Justin, Strate Jan, Li Cheng, Zhang Jian-Ming, Yu Wen-Jie, Di Zeng-Feng, Wang Xi
Chin. Phys. B, 2015, 24 (**11**): 118102. DOI: 10.1088/1674-1056/24/11/118102

Migration characterization of Ga and In adatoms on dielectric surface in selective MOVPE

Chen Wei-Jie, Han Xiao-Biao, Lin Jia-Li, Hu Guo-Heng, Liu Ming-Gang, Yang Yi-Bin, Chen Jie, Wu Zhi-Sheng, Liu Yang, Zhang Bai-Jun
Chin. Phys. B, 2015, 24 (**11**): 118101. DOI: 10.1088/1674-1056/24/11/118101

Transient thermal analysis as measurement method for IC package structural integrity

Alexander Hanß, Maximilian Schmid, E Liu, Gordon Elger
Chin. Phys. B, 2015, 24 (**6**): 068105. DOI: 10.1088/1674-1056/24/6/068105

A MOVPE method for improving InGaN growth quality by pre-introducing TMIn*

Zi-Kun Cao(曹子坤)[1,2], De-Gang Zhao(赵德刚)[1,3,†], Jing Yang(杨静)[1], Jian-Jun Zhu(朱建军)[1,3], Feng Liang(梁锋)[1], and Zong-Shun Liu(刘宗顺)[1]

[1] *State Key Laboratory of Integrated Optoelectronics, Institute of Semiconductors, Chinese Academy of Sciences, Beijing* 100083, *China*
[2] *College of Materials Science and Opto-Electronic Technology, University of Chinese Academy of Sciences, Beijing* 100049, *China*
[3] *Center of Materials Science and Optoelectronics Engineering, University of Chinese Academy of Sciences, Beijing* 100049, *China*

(Received 29 July 2020; revised manuscript received 28 August 2020; accepted manuscript online 14 September 2020)

We propose a metal organic vapor phase epitaxy (MOVPE) method of pre-introducing TMIn during the growth of u-GaN to improve the subsequent growth of InGaN and discuss the impact of this method in detail. Monitoring the MOVPE by the interference curve generated by the laser incident on the film surface, we found that this method avoided the problem of the excessive InGaN growth rate. Further x-ray diffraction (XRD), photoluminescence (PL), and atomic force microscope (AFM) tests showed that the quality of InGaN is improved. It is inferred that by introducing TMIn in advance, the indium atom can replace the gallium atom in the reactor walls, delivery pipes, and other corners. Hence the auto-incorporation of gallium can be reduced when InGaN is grown, so as to improve the material quality.

Keywords: InGaN, metal organic vapor phase epitaxy (MOVPE)

PACS: 81.05.Ea, 81.15.Gh, 78.70.Dm, 78.55.−m **DOI:** 10.1088/1674-1056/abb801

1. Introduction

The development of group III/V semiconductor materials is in the ascendant, and GaN-based optoelectronic materials are widely used in production. Especially the ternary alloy InGaN is extensively employed in the field of lasers and detectors. However, because of the mismatch between InN and GaN in the lattice, it is very difficult to grow high-quality InGaN. With the development of epitaxial technology, especially metal organic vapor phase epitaxy (MOVPE), the growth quality of InGaN has been improved. By studying the growth conditions and methods of MOVPE, we can better understand the growth mechanism of InGaN.

Due to the difference in the size of indium atoms and gallium atoms and the lattice mismatch between GaN and InN, the composition fluctuation and the phase separation may exist in InGaN due to low solubility between InN and GaN.[1,2] The growth of InGaN is particularly sensitive to temperature changes. Yoshimoto *et al.*[3,4] confirmed that in order to ensure the growth quality of InGaN crystals, the growth temperature of InGaN should be controlled to be relatively low at about 760 °C–800 °C. However, if the temperature is too low, indium atoms are easy to precipitate, resulting in poor overall quality. In order to reduce the problem of lattice mismatch, a layer of u-GaN should be grown at high temperatures before the growth of InGaN. Therefore, it is often to grow u-GaN at high temperatures first, and then cool down to grow InGaN.

It has been reported in many literatures that there is a memory effect of gallium during the growth of GaN. In other words, some gallium sources may remain on the reactor walls, delivery pipes, and other corners.[5–8] The quality of these unintentionally introduced sources is poor. Not only will a variety of impurities appear, but they may also exist in the form of polymer whose migration ability is very weak. These unintentional gallium sources act on the subsequent InGaN growth, thus reducing the material quality.

Based on the reasons mentioned above, we consider introducing TMIn into the growth of u-GaN. Because the activity of gallium is higher than that of indium, it can replace some unintentionally introduced gallium sources via

$$\mathrm{TMIn} + \mathrm{Ga} \rightarrow \mathrm{TMGa} + \mathrm{In}, \tag{1}$$

so as to improve the growth quality of InGaN materials.[9] In order to further study the influence of this method on material properties, we performed measurements of x-ray diffraction (XRD), photoluminescence (PL), and atomic force microscope (AFM) test on the two studied samples.

2. Growth of samples

The structure of the two studied samples is shown in Fig. 1. Sample 1 was grown using traditional methods, and sample 2 was grown by pre-introducing TMIn at 1100 °C at the end of u-GaN growth for about 1000 s. The conditions in the InGaN growth process of the two samples are exactly the same. Both samples are unintentionally doped, but due to

*Project supported by the National Key Research and Development Program of China (Grant Nos. 2016YFB0400803 and 2016YFB0401801) and the National Natural Science Foundation of China (Grant Nos. 61674138, 61674139, 61604145, 61574135, and 61574134).

†Corresponding author. E-mail: dgzhao@red.semi.ac.cn

the presence of impurities, these samples show weak n-type in InGaN.

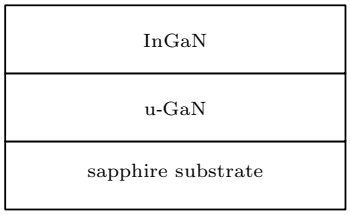

Fig. 1. The growth structure of two samples.

In the MOVPE growth process, for real-time monitoring, the growth condition was *in situ* tested by optical reflectivity using a He–Ne laser at 633 nm,[10–12] and the reflected laser intensity can provide information of the growth. Every time it oscillates, the thickness changes by $\frac{\lambda}{2n}$; each time from the highest point to the next lowest point, the thickness changes by $\frac{\lambda}{4n}$. Here λ is the wavelength of the laser, and n is the refractive index of the sample. In order to reduce the lattice mismatch, we grew a layer of u-GaN on a sapphire substrate at a growth temperature of about 1100 °C,[13,14] and then cooled down to about 800 °C for InGaN growth. Figure 2 depicts how the reflection intensity (black line) and the temperature (red line) change over time. It is seen that when the temperature drops to 800 °C, InGaN starts to grow. In Fig. 2(a), from arrow a to arrow c, it is exactly half a cycle, which takes 1129.2 s. According to Fig. 2(b), sample 2 goes from arrow e to arrow f, which takes 1900.5 s. It is shown that the growth rate of sample 2 is significantly reduced compared with that of sample 1. In Fig. 2(a), the height on Y-axis for arrow b and arrow d is the same. The position indicated by arrow c is the maximum point. The time duration from arrow b to arrow c is 707.7 s, and that from arrow c to arrow d is 1184.8 s. It can be seen that the

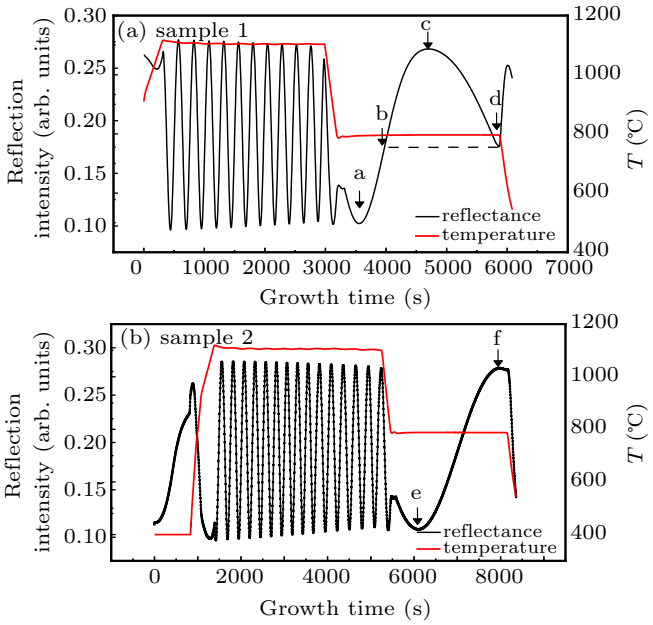

Fig. 2. The reflection intensity (black curve) and temperature (red curve) during the growth of (a) sample 1 and (b) sample 2.

initial growth rate of sample 1 is high, and then it slows down. The reason for this phenomenon is that the unintentionally introduced gallium is consumed as part of the gallium sources. Although the slope of the reflection curve cannot completely represent the growth rate, in general, the faster the half-cycle fluctuation is completed, the steeper the corresponding curve. That is, the average growth speed of InGaN by the traditional method is very fast in the initial stage. In summary, the new method of pre-introducing TMIn can indeed alleviate the problem of excessively fast conventional growth rates initially and can effectively stabilize the subsequent growth rate of InGaN.

3. Test and analysis

According to the research of Huang *et al.*,[13,15,16] the increase of gallium element leads to a dominating spiral growth mode.[17] In order to study the real effect of the new MOVPE method on InGaN growth, a series of tests, including XRD, PL, and AFM, were carried out. The test results are as follows.

3.1. XRD test

Two samples were measured at first by XRD. Figure 3 shows a ω–2θ scan at (002) planes. We can see only two apparent peaks in the logarithmic scale. InGaN peak is weak on the left, and GaN one on the right is relatively strong.[18] The values of the indium composition obtained from the simulation of the XRD curves are 5.964% for sample 1 and 6.615% for sample 2. Generally speaking, if the composition of indium increases, the quality of the material deteriorates. The lattice mismatch between InGaN and GaN can be further aggravated by higher indium composition.[19–22] However, the performance of sample 2 is better in subsequent tests, which further illustrates the good effect of the new method.

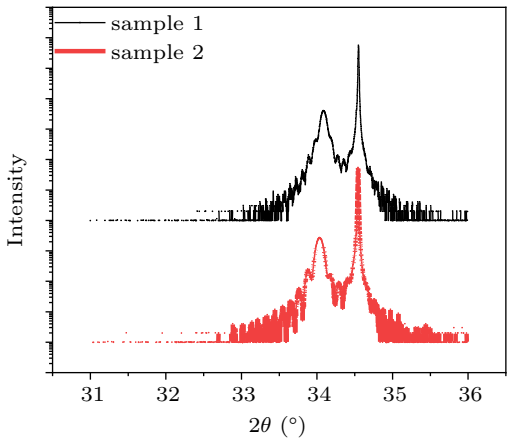

Fig. 3. The 2θ scan pattern of sample 1 and sample 2.

Through the curve fitting of XRD, we can also obtain that the thickness of the InGaN layer is 118.4 nm in sample 1 and 86.78 nm in sample 2.[23] Because the growth time of InGaN

of the two samples is the same, it can further prove that the average reaction rate is reduced by reducing the unintentional introduction of the gallium sources.

From the ω–2θ scan, it can be seen that both samples show apparent Pendellösung interference fringes near the main peak. If the crystal grows periodically, the light reflected from the upper and lower layers of each periodic structure is the source of Pendellösung interference fringes. Therefore, the better crystal interface, the more apparent Pendellösung interference fringes.[24,25] The diffraction peak of sample 2 in ω–2θ scanning is more obvious, which also indicates its better crystal quality.

To better reflect the dislocation of the materials, we also carried out ω scanning on the (002) plane of the two samples, and the results are shown in Fig. 4. The full width at half maximum (FWHM) is 296.86 arcsec for sample 1 and 293.79 arcsec for sample 2, which indicates that the edge dislocation of sample 2 is slightly smaller.[26]

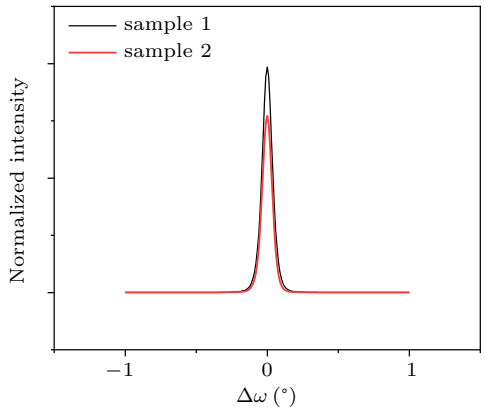

Fig. 4. The ω scan pattern of sample 1 and sample 2.

3.2. PL test

For further study the influence of the new method, we performed the PL test on the two samples. The 325 nm light form a helium–cadmium (He–Cd) laser was used for the measurement. Figures 5(a) and 5(b) show the PL curves of the two samples at 30 K. By fitting with the Gaussian function, the FWHMs are 9.679 nm for sample 1 and 9.296 nm for sample 2. Sample 2 has a narrower InGaN peak, which further indicates that its quality may be better.

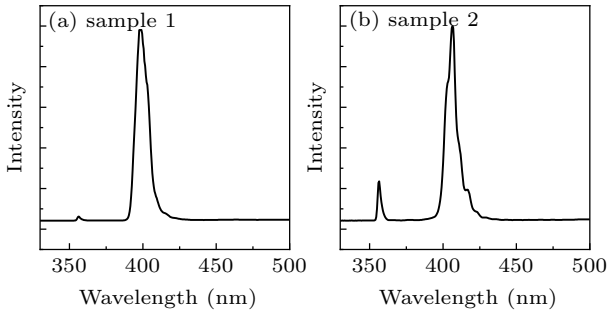

Fig. 5. PL curves of (a) sample 1 and (b) sample 2 at 30 K.

The peak energy for InGaN is about 3.0861 eV in sample 1 and 3.0331 eV in sample 2. The indium composition can be obtained from the Vegard law

$$E_{\mathrm{g}}^{\mathrm{In}_x\mathrm{Ga}_{1-x}\mathrm{N}} = (1-x)E_{\mathrm{g}}^{\mathrm{GaN}} + xE_{\mathrm{g}}^{\mathrm{InN}} - bx(1-x), \qquad (2)$$

where b is the bowing factor and is set as 1.43 eV. The indium composition obtained by formula (2) is 7.56% for sample 1 and 8.94% for sample 2.

The bowing factors reported in different literatures are slightly different.[27–30] The result suggests that after the pre-introducing of indium, the chamber cavity also has more residual indium source, which causes the indium composition to increase.[13,14,31,32] Actually, the composition results of PL are basically consistent with the XRD ones.

3.3. AFM test

In order to further study the changes in sample quality brought by the new method, the AFM test was performed on the two samples. Figure 6 shows the AFM scan (2×2 μm^2) image in the central area. It can be seen that both samples have obvious two-dimensional step flow growth, indicating that the growth quality is relatively high. At the same time, V-shaped pits unique to InGaN samples appear. The root mean square (RMS) roughness is 0.574 nm for sample 1 and 0.293 nm for sample 2.[33] It can be seen that sample 2 shows a smoother appearance. A deeper analysis through the software provided by the AFM instrument shown in Fig. 7 can also indicate that the performance of InGaN near the surface should be better in sample 2.

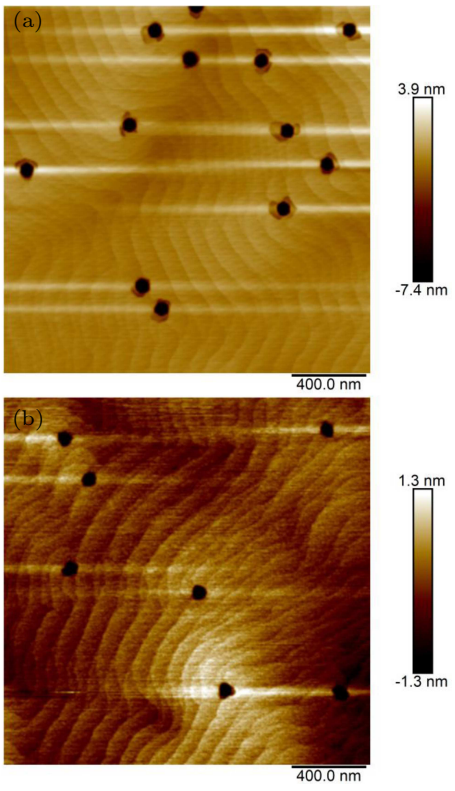

Fig. 6. AFM images of (a) sample 1 and (b) sample 2.

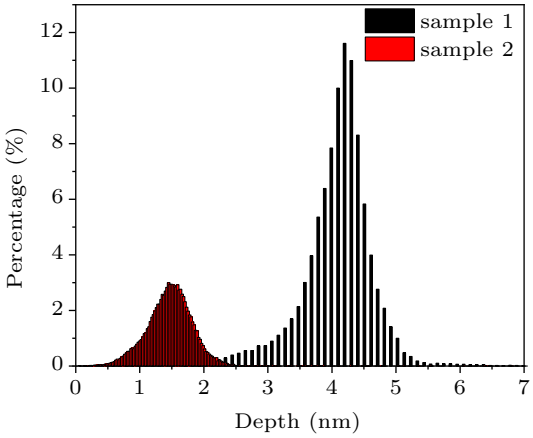

Fig. 7. The distribution of depth in sample 1 and sample 2.

4. Conclusion

Through the growth curve of the *in situ* reflected light, it can be seen that the method of pre-introducing TMIn can effectively solve the problem of the excessively fast InGaN material growth rate. For sample 2, which is grown using the new method, the FWHM values of both PL peak at 30 K and XRD omega scan are slightly smaller, and Pendellösung interference fringes in the ω–2θ scan are more obvious. Moreover, the AFM test shows a smaller RMS and a lower depth distribution. All these indicate that sample 2 owns a higher quality. In particular, sample 2 has a higher indium composition but still has a higher material quality, which demonstrates the advantages of this pre-introducing TMIn method.

References

[1] Ho I H and Stringfellow G B 1996 *Appl. Phys. Lett.* **69** 2701
[2] Karpov S Y 1998 *MRS Internet J. Nitride Semicond. Res.* **3** 16
[3] Yoshimoto N, Matsuoka T, Sasaki T and Katsui A 1991 *Appl. Phys. Lett.* **59** 2251
[4] Wang D H, Xu S R, Zhang J C, Chen K, Bi Z W, Zhang L X, Meng F N, Ai S and Hao Y 2012 *Journal of the Korean Physical Society* **61** 618
[5] Taylor E, Smith M D, Sadler T C, Lorenz K, Li H N, Alves E, Parbrook P J and Martin R W 2014 *J. Cryst. Growth* **408** 97
[6] Choi S, Jin Kim H, Lochner Z, Kim J, Dupuis R D, Fischer A M, Juday R, Huang Y, Li T, Huang J Y, Ponce F A and Ryou J H 2014 *J. Cryst. Growth* **388** 137
[7] Kim J, Lochner Z, Ji M H, Choi S, Kim H J, Kim J S, Dupuis R D, Fischer A M, Juday R, Huang Y, Li T, Huang J Y, Ponce F A and Ryou J H 2014 *J. Cryst. Growth* **388** 143
[8] Zhu J J, Fan Y M, Zhang H, Lu G J, Wang H, Zhao D G, Jiang D S, Liu Z S, Zhang S M, Chen G F, Zhang B S and Yang H 2012 *J. Cryst. Growth* **348** 25
[9] Hiroki M, Oda Y, Watanabe N, Maeda N, Yokoyama H, Kumakura K and Yamamoto H 2013 *J. Cryst. Growth* **382** 36
[10] Wen F, Huang L R, Jiang B, Tong L Z, Xu W and Liu D 2010 *J. Semicond.* **31** 094010
[11] Brunner F, Hoffmann V, Knauer A, Steimetz E, Schenk T, Zettler J T and Weyers M 2007 *J. Cryst. Growth* **298** 202
[12] Zhu D, McAleese C, McLaughlin K K, Häberlen M, Salcianu C O, Thrush E J, Kappers M J, Phillips W A, Lane P, Wallis D J, Martin T, Astles M, Thoms S, Pakes A, Heuken M and Humphreys C J 2009 *Light-Emitting Diodes: Materials, Devices, and Applications for Solid State Lighting XIII* **7231** 723118
[13] Huang Y, Melton A, Jampana B, Jamil M, Ryou J H, Dupuis R D and Ferguson I T 2011 *J. Appl. Phys.* **110** 064908
[14] Tao T, Zhang Z, Liu L, Su H, Xie Z, Zhang R, Liu B, Xiu X, Li Y, Han P, Shi Y and Zheng Y 2011 *Journal of Semiconductors* **32** 14
[15] Ema K, Uei R, Murakami H and Koukitu A 2019 *Jpn. J. Appl. Phys.* **58** 1027
[16] Liu Z, Nitta S, Usami S, Robin Y, Kushimoto M, Deki M, Honda Y, Pristovsek M and Amano H 2019 *J. Cryst. Growth* **509** 50
[17] Yang J, Liu S T, Wang X W, Zhao D G, Jiang D S, Chen P, Zhu J J, Liu Z S, Liang F, Liu W, Zhang L Q, Yang H, Wang W J and Li M 2018 *Superlattices Microstruct.* **113** 34
[18] Qin Z, Chen Z, Tong Y, Lu S and Zhang G 2002 *Appl. Phys. A* **74** 655
[19] Li Q and Wang G T 2010 *Appl. Phys. Lett.* **97** 2701
[20] Soto Rodriguez P E D, Gómez V J, Kumar P, Calleja E and Nötzel R 2013 *Appl. Phys. Lett.* **102** 131909
[21] Fu S F, Chen C Y, Li F W, Hsu C H, Chou W C, Chang W H, Chen W K and Ke W C 2013 *J. Cryst. Growth* **383** 106
[22] Choi S B, Shim J P, Kim D M, Jeong H I, Jho Y D, Song Y H and Lee D S 2013 *Appl. Phys. Lett.* **103** 033501
[23] Chen Z T, Tan S X, Sakai Y and Egawa T 2009 *Appl. Phys. Lett.* **94** 213504
[24] Singh S D, Patra N, Singh M N, Mukherjee C, Jha S N, Sinha A K and Ganguli T 2018 *Journal of Materials Science* **54** 1992
[25] Althowibi F A and Ayers J E 2017 *J. Electron. Mater.* **47** 1158
[26] Lee H J, Baek S H, Na H and Lee S N 2019 *Journal of the Korean Physical Society* **75** 362
[27] Wu J, Walukiewicz W, Yu K M, Ager J W, Haller E E, Lu H and Schaff W J 2002 *Appl. Phys. Lett.* **80** 4741
[28] Schley P, Goldhahn R, Winzer A T, Gobsch G, Cimalla V, Ambacher O, Lu H, Schaff W J, Kurouchi M, Nanishi Y, Rakel M, Cobet C and Esser N 2007 *Phys. Rev. B* **75** 205204
[29] Hori M, Kano K, Yamaguchi T, Saito Y, Araki T, Nanishi Y, Teraguchi N and Suzuki A 2002 *Phys. Stat. Sol. (b)* **234** 750
[30] McCluskey M D, Van de Walle C G, Romano L T, Krusor B S and Johnson N M 2003 *J. Appl. Phys.* **93** 4340
[31] Kim H J, Na H, Kwon S Y, Seo H C, Kim H J, Shin Y, Lee K H, Kim D H, Oh H J, Yoon S, Sone C, Park Y and Yoon E 2004 *J. Cryst. Growth* **269** 95
[32] Shrestha N M, Chauhan P, Wong Y Y, Li Y, Samukawa S and Chang E Y 2020 *Vacuum* **171** 108974
[33] Vickers M E, Kappers M J, Smeeton T M, Thrush E J, Barnard J S and Humphreys C J 2003 *J. Appl. Phys.* **94** 1565